Contributed paper

OPTO-ELECTRONICS REVIEW 9(1), 83–90 (2001)

# Spectral and generation characteristics of YAG:$Nd^{3+}$ crystals with high concentration of $Nd^{3+}$ ions

Z. MIERCZYK*[1], K. KOPCZYŃSKI[1], W. ŻENDZIAN[1], and T. ŁUKASIEWICZ[2]

[1]Institute of Optoelectronics, Military University of Technology
2 Kaliskiego Str., 00-908 Warsaw, Poland
[2]Institute of Electronic Materials Technology, 133 Wólczyńska Str., 01-919 Warsaw, Poland

*The paper presents investigation results of optical, spectroscopic, and generation parameters of YAG:$Nd^{3+}$ with higher concentration of $Nd^{3+}$ ions (1.1–1.8 at. % $Nd^{3+}$). YAG:$Nd^{3+}$ single crystals were obtained by the Czochralski method. Investigations on optical quality were carried out using elastoscopic and interferometric methods. Absorption spectra within the spectral range of 200–3000 nm ($\Delta\lambda$ = 1 nm) and pumping range of 750–850 nm ($\Delta\lambda$ = 0.1 nm) were determined. Also the spectra of luminescence induced with radiation emitted by a laser diode of 808 nm were investigated and lifetime of $Nd^{3+}$ ions in the upper laser level ($^4F_{3/2}$) was determined. In the all investigated crystals, doped up to 1.3 at.% $Nd^{3+}$, the time of fluorescence decay from $^4F_{3/2}$ level is 230 µs. It was stated that high level of $Nd^{3+}$ ions doping (above 1.33 at. % $Nd^{3+}$) causes reduction of lifetime of the upper level $^4F_{3/2}$ as a result of concentric quenching of luminescence. For the crystals of 1.8 at. % $Nd^{3+}$ concentration, upper laser level lifetime has been reduced to 183 µs. Also the results of generation investigations obtained in a laser system with the examined YAG:$Nd^{3+}$ active media in form of side pumped "slabs" and in form of longitudinally pumped rod.*

**Keywords:** crystal growth, YAG:$Nd^{3+}$, diode pumped solid state lasers, microlasers, giant-pulse lasers.

## 1. Introduction

Solid-state lasers with a selective laser diode pumping create a new family of lasers having special features and wide applicability. Due to spectral matching of radiation emitted by laser diodes to absorption bands of active medium it is possible to obtain high efficiency of pumping, single mode generation, and excitation of very small-sized media. In order to increase pumping efficiency, the media having lattices ensuring high level of doping with activation ions are used. High level of doping with activator ions causes extension of absorption bands in pumping region. As a result, the output parameters of the whole laser system are less sensitive to thermal drift of wavelength (≈0.3 nm/K) generated by a diode laser. Doping level is limited in many materials by the processes of concentric quenching of luminescence that reduced lifetime of laser upper level. Optimal doping is usually a compromise between pumping efficiency and lifetime of the upper laser level.

From among many investigated ions-activators in various crystalline lattices the most frequently used are the lasers with active media doped with neodymium ions. Analysis of absorption spectra allows for estimation of diode pumping of these media. The basic evaluation criteria are the value of absorption coefficient and width of absorption band within wavelengths of pumping laser diode. A value of absorption coefficient is crucial for pumping efficiency and width of absorption band determines the range of required thermal stabilisation of a laser diode.

Doping level in commonly used YAG:$Nd^{3+}$ crystals does not exceed 1–1.1 at. % $Nd^{3+}$ [1,2]. A structure of yttrium aluminium garnet is not favourable for higher neodymium concentrations. Large radius of $Nd^{3+}$ ion makes it difficult to occupy yttrium positions in oxygen dodecahedrons. A coefficient of dopant distribution is ~ 0.2 what also makes it difficult to have YAG:$Nd^{3+}$ single crystals of high and homogeneous concentration of $Nd^{3+}$ ions.

The aim of the carried out works was to obtain YAG:$Nd^{3+}$ single crystals of higher concentration of $Nd^{3+}$ ions devoted to diode pumped microlasers. High concentration of activator ions ensures strong absorption of pump radiation causing reduction of active medium's length. Because of a small size of active medium, the cavity mode spacing (which is inversely proportional to the cavity length) is comparable to the gain bandwidth of the lasing transition. In such a system a single longitudinal mode is generated what is significant for its applicability [3].

## 2. Crystal growth

*e-mail: zmierczy@wat.waw.pl

The YAG:Nd$^{3+}$ single crystals were obtained by the Czochralski method, using iridium crucibles of external dimensions ϕ 50×50×1.5 mm. Insulating housing of the crucible was made of alundum ceramics and granular zirconium ceramics, stabilised with hafnium ($ZrO_2$:$HfO_2$), that filled the space between the crucible, the tube, and alundum base. The crystallisation processes were carried out in nitrogen atmosphere containing small amount (a fraction of percentage) of oxygen. High purity oxides $Y_2O_3$ (5N) and $Al_2O_3$ (5N) from J.M.&PROD., $Nd_2O_3$ (5N) from ALDRICH were used as initial materials.

YAG:Nd$^{3+}$ crystals of concentrations from 1.1 at. % to 1.76 at. % Nd$^{3+}$ and diameter of about 25 mm and length 60 mm were obtained. In all the crystals, a core area of the characteristic threefold symmetry was found. The core has clear, sharp boundaries and its area has a diameter of about 2 mm. On the basis of the investigations carried out with a Mach-Zender interferometer it was stated that values of refractive index in the crystal's core area are various due to defects and stresses. Thus, the whole crystals were optically homogeneous excluding the core area. Characteristic interferograms obtained for a YAG:Nd$^{3+}$ crystal No. 2 of 1.35 at. % Nd$^{3+}$ are shown in Fig. 1.

The stresses in crystals were examined using elastoscopic method and registering the picture obtained for investigated crystal, placed between crossed polarisers. Figure 2 shows the results for YAG:Nd$^{3+}$ crystal No. 2.

On the basis of the interferometric and elastoscopic investigations the areas of the crystal cuts were determined in order to perform optical elements for investigations of spectroscopic characteristics.

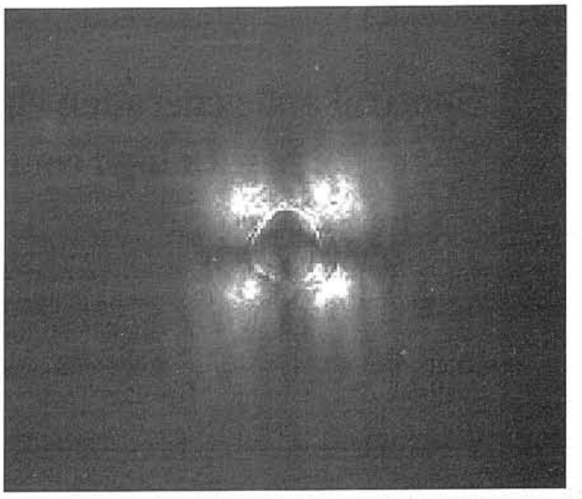

Fig. 2. Elastoscopic picture obtained for the YAG:Nd$^{3+}$ crystal No. 2 of a length 50 mm.

## 3. Spectroscopic investigations

From the obtained crystals the plane-parallel plates of 1 mm thickness were cut and polished for measurements of spectral characteristic. In order to determine a dependence of the absorption coefficient on wavelength k(λ) of the investigated samples, the transmission was measured as a function of the wavelength. The measurements were carried out within the spectral range of 200–3000 nm ($\Delta\lambda$ = 1 nm) and 750–850 nm ($\Delta\lambda$ = 0.1 nm) using a LAMBDA 900 PERKIN ELMER spectrophotometer.

On the basis of transmission measurements of T(λ) samples, the absorption coefficient was calculated regarding multiple radiation reflections inside a sample.

Concentration of $N_{Nd^{3+}}$ ions was determined according to approximate relationship

$$k_{808}(cm^{-1}) = N_{Nd^{3+}}\sigma_{808}, \qquad (1)$$

where $k_{808}$ is the absorption coefficient for $\lambda$ = 808 nm and $\sigma_{808}$ is the absorption cross-section ($\sigma_{808} = 5\times10^{-20}$ cm$^2$). So

$$N_{Nd^{3+}} = 2k_{808}\times10^{19}(cm^{-3}). \qquad (2)$$

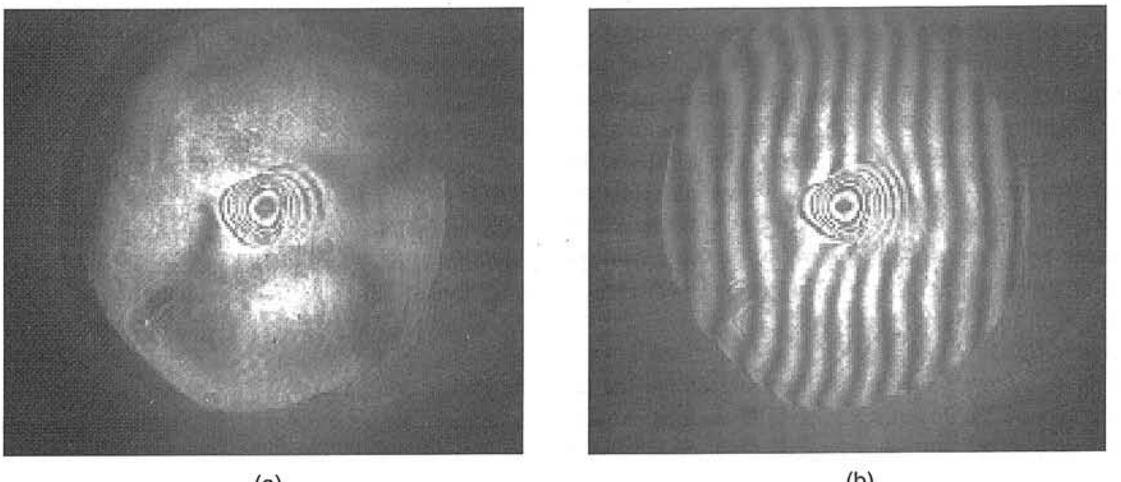

(a) (b)

Fig. 1. Interferograms obtained for YAG:Nd$^{3+}$ crystal No. 2 of a length 50 mm: (a) zero-fring order and (b) multi-fring field.

 

Percentage content (% at.) of neodymium ions in a particle of $Nd^{3+}$ doped yttrium-aluminium garnet $Y_{3(1-x)}Nd_{3x}Al_5O_{12}$ can be determined from the relationship

$$N_{Nd^{3+}} = \frac{\rho N_A 3x}{M}, \quad (3)$$

where ρ is the density of YAG:$Nd^{3+}$ crystal, ρ = 4.56 g/cm$^3$, x is $Nd^{3+}$ concentration (at. %) and $N_A$ is the Avogadro's number, $N_A$ = 6.022169×10$^{23}$ mol$^{-1}$, M is the molecular weight $Y_{3(1-x)}Nd_{3x}Al_5O_{12}$, M = 593.618 + 1.660x.

For 1.0 at % contents of $Nd^{3+}$, the concentration of $N_{Nd^{3+}}$

$$N_{Nd^{3+}} = \frac{\rho N_A 3x}{593.618 + 1.660x} \quad (4)$$

is 1.388×10$^{20}$ cm$^{-3}$ Thus, percentage content of neodymium ions can be estimated from the relationship

$$x(\%\ at.) = \frac{593.618 N_{Nd^{3+}}}{3\,(\rho N_A - 1.660 N_{Nd^{3+}})} = \frac{593.618 \dfrac{k_{808}}{\sigma_{808}}}{3\left(\rho N_A - 1.660 \dfrac{k_{808}}{\sigma_{808}}\right)}. \quad (5)$$

Table 1. Basic spectroscopic parameters of the selected YAG:$Nd^{3+}$ samples.

| No. | Sample | k (808 nm) (cm$^{-1}$) | $N_{Nd^{3+}}$(×10$^{-20}$) (cm$^{-1}$) | k (1064 nm) (cm$^{-1}$) | $Nd^{3+}$ concentration (at.%) | |
|---|---|---|---|---|---|---|
| | | | | | Calculations | Chemical analysis |
| 1 | YND1P01 | 8.31 | 1.66 | 0.012 | 1.20 | 1.2 |
| 2 | YND1P02 | 7.70 | 1.54 | 0.037 | 1.11 | 1.1 |
| 3 | YND2P01 | 8.29 | 1.66 | 0.041 | 1.19 | 1.2 |
| 4 | YND2P02 | 8.29 | 1.66 | 0.061 | 1.19 | 1.2 |
| 5 | YND3P01 | 9.26 | 1.85 | 0.005 | 1.33 | 1.3 |
| 6 | YND3P02 | 9.37 | 1.87 | 0.009 | 1.35 | 1.3 |
| 7 | YND3P03 | 9.26 | 1.85 | 0.011 | 1.33 | 1.3 |
| 8 | YND3P04 | 9.02 | 1.80 | 0.002 | 1.30 | 1.3 |
| 9 | YND4P01 | 8.90 | 1.78 | 0.004 | 1.28 | 1.3 |
| 10 | YND4P02 | 9.22 | 1.84 | 0.007 | 1.33 | 1.3 |
| 11 | YND5P01 | 8.60 | 1.72 | 0.073 | 1.24 | 1.2 |
| 12 | YND5P02 | 9.24 | 1.84 | 0.037 | 1.33 | 1.3 |
| 13 | YND5P03 | 8.20 | 1.64 | 0.070 | 1.18 | 1.1 |
| 14 | YND5P04 | 8.36 | 1.68 | 0.116 | 1.21 | 1.2 |
| 15 | YND6P01 | 8.73 | 1.50 | 0.003 | 1.25 | 1.2 |
| 16 | YND6P02 | 8.78 | 1.36 | 0.006 | 1.27 | 1.2 |
| 17 | YND6P03 | 8.33 | 1.26 | 0.004 | 1.20 | 1.2 |
| 18 | YND6P04 | 8.14 | 1.28 | 0.004 | 1.17 | 1.2 |
| 19 | YND7P01 | 10.36 | 2.08 | 0.003 | 1.50 | 1.5 |
| 20 | YND7P02 | 10.28 | 2.06 | 0.073 | 1.48 | 1.5 |
| 21 | YND7P03 | 9.29 | 1.86 | 0.061 | 1.34 | 1.3 |
| 22 | YND7P04 | 9.59 | 1.92 | 0.039 | 1.38 | 1.4 |
| 23 | YND8P01 | 12.24 | 2.44 | 0.042 | 1.76 | 1.8 |
| 24 | YND8P02 | 12.00 | 2.40 | 0.003 | 1.73 | 1.7 |
| 25 | YND8P03 | 11.39 | 2.28 | 0.085 | 1.64 | 1.7 |
| 26 | YND8P04 | 10.85 | 2.20 | 0.123 | 1.59 | 1.6 |

The measurement results of spectroscopic parameters and calculation results of $Nd^{3+}$ ions concentration obtained for the selected samples are listed in Table 1. Table 1 presents also the results of chemical analysis made for the same samples in order to determine $Nd^{3+}$ ions concentration. As it can be seen, $Nd^{3+}$ concentrations, calculated according to the assumed approximation, were confirmed by the results of chemical analysis.

Optical quality of a crystal can be determine by its absorption coefficient within a generation region (1064 nm).

Laser induced luminescence was recorded in L20 (JOBIN YVON) monochromator with LOCK-IN (STANFORD RESEARCH SR510) system with thermoelectrically cooled InGaAs detector. Relative luminescence intensities for the selected samples of YAG:$Nd^{3+}$ monocrystals of various $Nd^{3+}$ concentration are presented in Table 2.

Also there were carried out measurements of $Nd^{3+}$ ions lifetimes in the upper laser level $^4F_{3/2}$ for YAG:$Nd^{3+}$ samples made from the investigated crystals. The measurements were carried out by a direct method using pulse excitation.

In this method, the investigated medium is excited with pulse radiation of a pulse duration significantly shorter than the lifetime $\tau$ in the excitation level. A source of diagnostic pulses was the laser diode SDL2432 supplied with SDL800 power supplier, controlled by a pulse generator. The laser generated the pulses of wavelength 808 nm, duration 7.8 μs, and frequency ~0.66 kHz. Silicon photodiode was used in a detection path, perpendicular to the excitation path. Temporal characteristics of fluorescence decay were recorded using LeCROY 9350AM (500 MHz) digital oscilloscope. The measurement results of fluorescence decay time in the investigated samples are given in Table 2.

Table 2. Measurement results of fluorescence decay time for YAG:$Nd^{3+}$ samples.

| Crystal No. | $Nd^{3+}$ ions concentration (at. %) | Fluorescence intensity (a.u.) | $\tau$ (μs) | $\Delta\tau$ (μs) |
|---|---|---|---|---|
| 1 | 1.10 | 65 | 236 | ±5 |
| 2 | 1.35 | 99 | 231 | ±5 |
| 3 | 1.30 | 78 | 238 | ±5 |
| 4 | 1.35 | 75 | 217 | ±5 |
| 5 | 1.33 | 85 | 210 | ±5 |
| 6 | 1.27 | 95 | 215 | ±5 |
| 7 | 1.50 | 100 | 201 | ±5 |
| 8 | 1.76 | 99 | 183 | ±5 |

Figure 3 presents the results of fluorescence decay from the level $^4F_{3/2}$ obtained for YAG:$Nd^{3+}$ of various concentration of $Nd^{3+}$ ions.

As it is shown from the obtained results, in all investigated crystals, doped to 1.3% at. $Nd^{3+}$, fluorescence decay

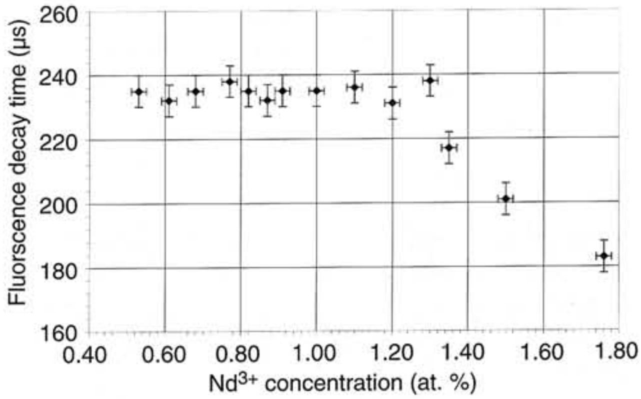


Fig. 3. Influence of $Nd^{3+}$ ions concentration in YAG:$Nd^{3+}$ crystals on fluorescence decay from $^4F_{3/2}$ level.

from the level $^4F_{3/2}$ is about 230 μs. High level of $Nd^{3+}$ ions doping (above 1.3 at. % $Nd^{3+}$) causes reduction of lifetime of the upper laser level $^4F_{3/2}$ due to concentric luminescence decay.

## 4. Generation investigations

In order to examine the influence of high doping level of YAG:$Nd^{3+}$ on generation characteristics of a diode pumped laser, active elements made from the investigated YAG:$Nd^{3+}$ crystals, pumped longitudinally with CW laser diode, generating in CW regime and with passively Q-switched resonator. A scheme of the measuring system is shown in Fig. 4. Laser diode SDL 2362 P3 with the fibre output (optical waveguide 50 μm) of the output power up to 0.7 W was used. The diode was supplied with SDL 822 power supply having temperature control system. The output power was measured using Rm 6600 Laser Precission Corp. meter with RKP-575 probe and for investigations of spatial characteristics of generated radiation the CCD 480×640 matrix with FRAME-GRABER card was used.

Generation investigations of longitudinally pumped microlasers, made of YAG:$Nd^{3+}$ with various $Nd^{3+}$ ions concentration, were carried out. The measuring results are presented in Fig. 5. This figure shows comparison of generation characteristics of four microlasers, 4 mm in diameter, made of YAG:$Nd^{3+}$ crystals with various concentration of $Nd^{3+}$ ions. Table 3 presents basic parameters of the examined active elements made from four various YAG:$Nd^{3+}$ crystals. Also the generation characteristics of longitudinally CW pumped microlasers with passive Q-switching, generating giant-pulses with high repetition rate were investigated.

Figure 6 shows exemplary generation characteristics of microlaser in which active element made from YAG:$Nd^{3+}$ crystal No. 7 of 1.5% at. $Nd^{3+}$ concentration and passive Q-switch YAG:$Cr^{4+}$ of initial transmission 85.6%. Figures 7, 8, and 9 show the generation oscillograms of giant pulses series through this microlaser for various pumping powers. As it can be seen from the obtained data, increase in pump

 

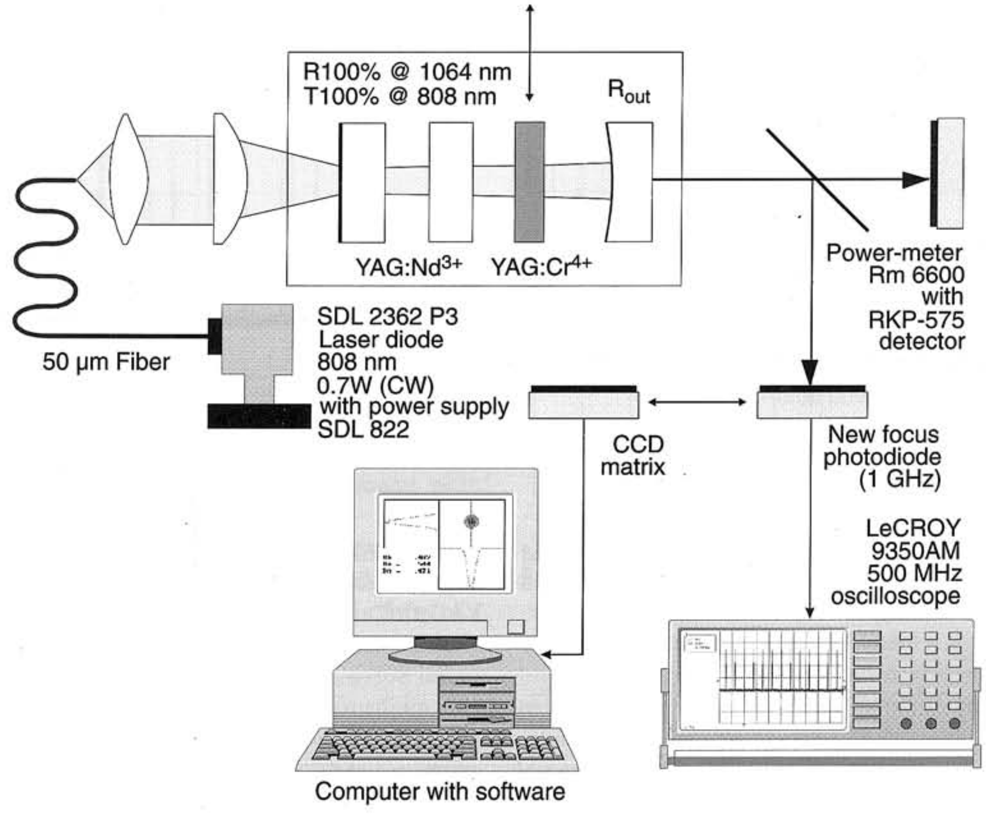


Fig. 4. Scheme of measuring system for investigation of active elements made from the examined YAG:$Nd^{3+}$ crystals, pumped longitudinally with CW diode laser generating in CW regime and with passive Q-switching.

power causes increase in average power generated by the microlaser due to increase of repetition rate. Stable passive Q-switching generation of giant-pulses series of various frequency, for constant duration of single monopulse has been obtained. Figure 10 shows an oscillogram of 16-ns giant-pulse.

Table 4 presents the results of investigations on Q-switching generation. Giant-pulses were generated due to longitudinally CW pumped YAG:$Nd^{3+}$ microlasers of various $Nd^{3+}$ ions concentration with YAG:$Cr^{4+}$ modulator.

Table 3. Basic parameters of the investigated active elements made from four various YAG:$Nd^{3+}$ crystals.

| Active element | YAG:$Nd^{3+}$ crystal No. | Thickness (mm) | $Nd^{3+}$ concentration (at.%) |
|---|---|---|---|
| YND5A01 | 5 | 1.817 | 1.20 |
| YND6A01 | 6 | 1.818 | 1.25 |
| YND7A01 | 7 | 1.817 | 1,50 |
| YND8A01 | 8 | 1.825 | 1.75 |

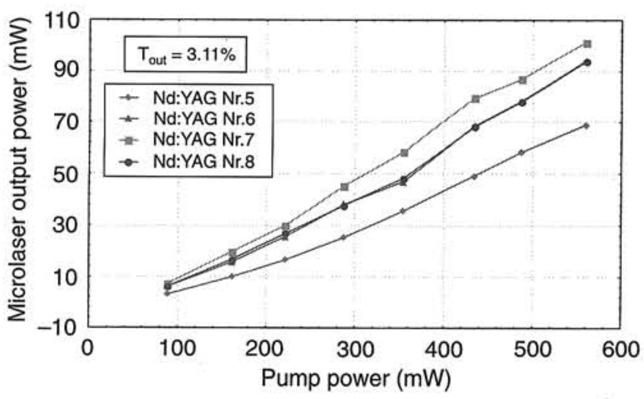


Fig. 5. Comparison of generation characteristics of four microlasers, 4 mm in diameter, made from YAG:$Nd^{3+}$ crystals of various concentration of $Nd^{3+}$ ions.

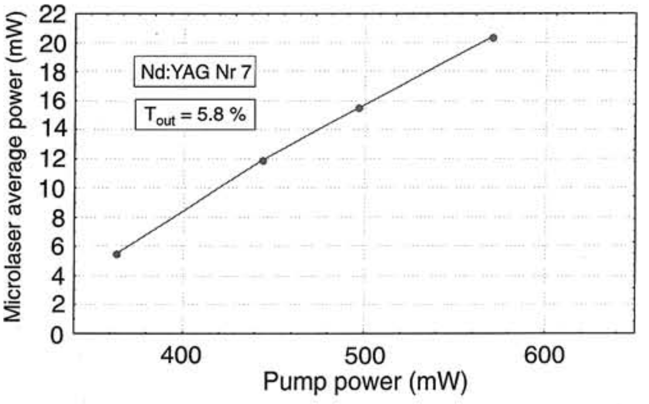


Fig. 6. Results of generation investigations of YAG:$Nd^{3+}$ microlaser with YAG:$Cr^{4+}$ modulator for optimal transmission of the output mirror.

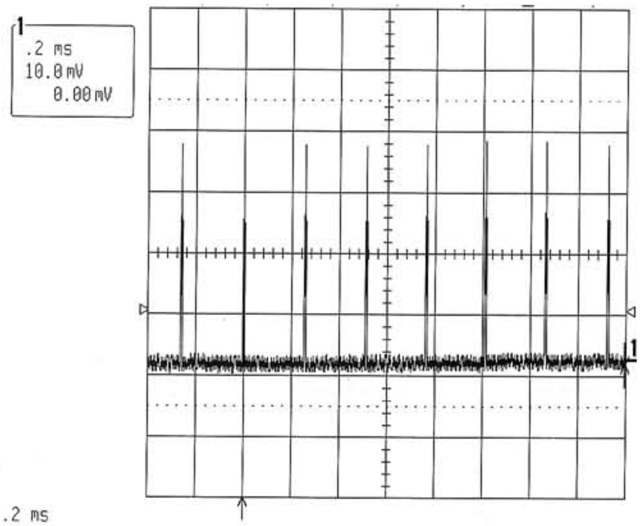


Fig. 7. Oscillogram of giant pulses series generation obtained due to longitudinally CW pumped YAG:$Nd^{3+}$ microlaser with YAG:$Cr^{4+}$ modulator. $P_{in}$ = 443 mW, $P_{out}$ = 10.1 mW, $\tau_{1/2}$ = 16 ns.

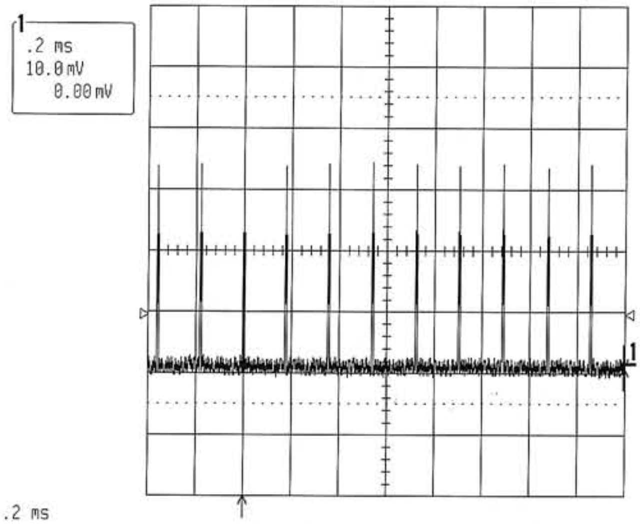


Fig. 8. Oscillogram of giant pulses series generation obtained due to longitudinally CW pumped YAG:$Nd^{3+}$ microlaser with YAG:$Cr^{4+}$ modulator. $P_{in}$ = 497 mW, $P_{out}$ = 16.7 mW, $\tau_{1/2}$ = 16 ns.

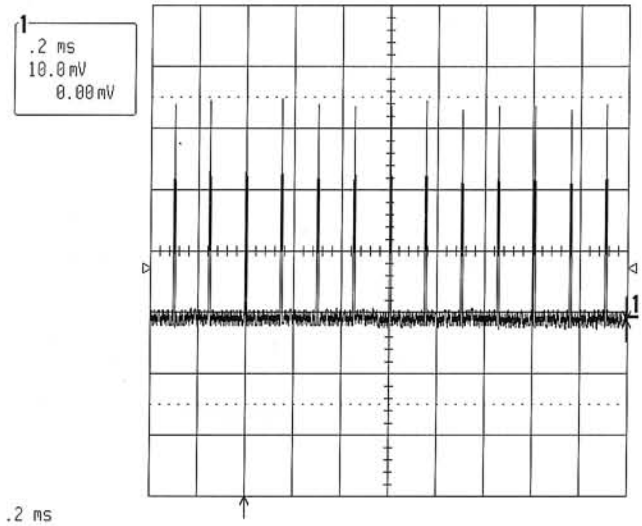


Fig. 9. Oscillogram of giant pulses series generation obtained due to longitudinally CW pumped YAG:$Nd^{3+}$ microlaser with YAG:$Cr^{4+}$ modulator. $P_{in}$ = 570 mW, $P_{out}$ = 20.4 mW, $\tau_{1/2}$ = 16 ns.

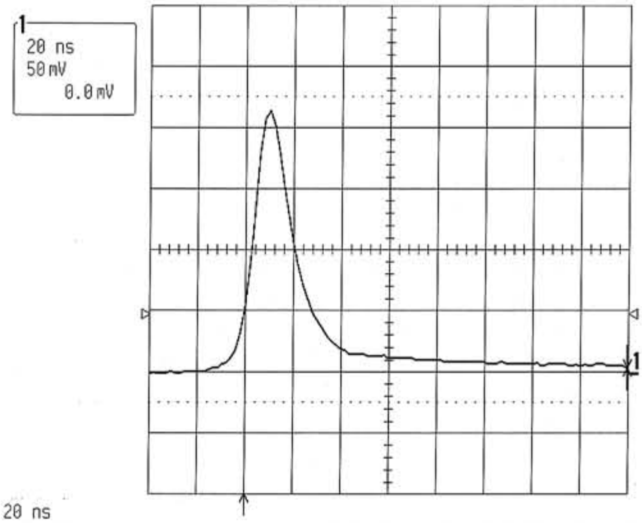


Fig. 10. Oscillogram of single giant pulse of half-width duration of 16 ns of giant pulses series, generated by longitudinally CW pumped YAG:$Nd^{3+}$ microlaser with YAG:$Cr^{4+}$ modulator.

Table 4. Investigation results of giant pulses series due to longitudinally CW pumped YAG:$Nd^{3+}$ microlasers of various concentration of $Nd^{3+}$ ions with YAG:$Cr^{4+}$ modulator. Input power $P_{in}$ = 570 mW, initial transmission YAG:$Cr^{4+}$ $T_0$ = 85.6%, transmission of the output mirror T = 5.8%.

| Active element | YAG:$Nd^{3+}$ crystal No. | $Nd^{3+}$ (at. %) concentration | Output power $P_{out}$ (mW) | Repetition rate (kHz) | Giant-pulse duration $\tau_{1/2}$ (ns) |
|---|---|---|---|---|---|
| YND5A01 | 5 | 1.20 | 10.1 | 3.7 | 16 |
| YND6A01 | 6 | 1.25 | 16.7 | 4.5 | 16 |
| YND7A01 | 7 | 1.50 | 20.4 | 6.7 | 16 |
| YND8A01 | 8 | 1.75 | 14.2 | 4.8 | 16 |

 

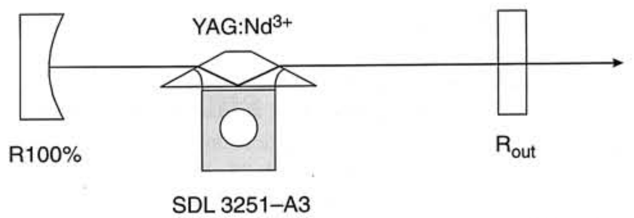


Fig. 11. Scheme of Nd:YAG laser side pumped with 300 W laser diode with active medium in form of triangular "slab". R100% is the totally reflected mirror of radius curvature 2000 mm, $R_{out}$ is the plane output mirror of transmission 15%.

Also generation investigations of active element made from the examined crystals in side pumped system were carried out. The investigations were made for the laser having configuration shown in Fig. 11. Active elements were made as single reflected "slabs".

Generation characteristics of the above laser were measured for the slabs denoted SL1/1, SL1/2, SL3/1, SL3/2, SL3/3, SL3/4 and TR. All the slabs were made in form of a triangle with a truncated vertex. On a truncation surface, the totally reflected layer was deposited for $\lambda = 808$ nm to use a part of radiation that is not absorbed in a medium during the first radiation transition. From the pump's side, the slabs were covered with an antireflection layer for wavelength $\lambda = 808$ nm.

The slabs were situated in a resonator, in such a way that they were in direct contact with the laser diode's surface. Each replacement of the slab caused necessity of insignificant resonator alignment to the maximal output energy. Energetic characteristics of the carried out measurements are presented in Fig. 12.

Table 5 presents the values of generation efficiency and maximal generation energies of the investigated laser elements.

The investigated elements, made from YAG:$Nd^{3+}$ crystals of higher $Nd^{3+}$ concentration, can be divided into two groups: the first includes the slabs SL1/1, SL3/1 and TR, and the second one the slabs SL1/2, SL3/2, SL1/3, SL3/4. The highest generation efficiency was obtained for active elements made from YAG:$Nd^{3+}$ crystals of concentration below 1.3 at. % $Nd^{3+}$. It testifies to influence of high doping on optical quality and homogeneity of YAG:$Nd^{3+}$ crystals. This effect did not occur when very small active elements were used.

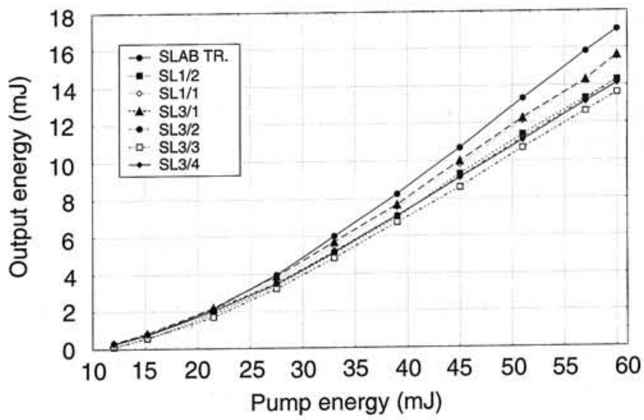


Fig. 12. Energetic characteristics of a laser with the investigated active YAG:$Nd^{3+}$ elements

## 5. Conclusions

The growth conditions of YAG:$Nd^{3+}$ single crystals, of higher $Nd^{3+}$ concentration from 1.33% at. to 1.76% at., have been determined. High level of $Nd^{3+}$ ions doping (above 1.33% at. $Nd^{3+}$) caused reduction of lifetime of the upper laser level $^4F_{3/2}$ as a result of concentric luminescence quenching. In the all investigated crystals, doped up to 1.3 at. % $Nd^{3+}$, the fluorescence decay time from $^4F_{3/2}$ level was ~230 μs

As it results from the carried out investigations of active elements made from YAG:$Nd^{3+}$ single crystals of higher $Nd^{3+}$ ions concentration (above 1.5 at. %), in the system of longitudinally CW pumped laser, generating giant pulses series, one can observe the decrease of power output of the microlaser both in CW regime and with passive Q-switching.

In the active elements, made in form of "slabs", energetic laser characteristics were worse for $Nd^{3+}$ ions concentration of above 1.3 at. %.

The investigations of optical and spectroscopic properties of the obtained monocrystals showed their high optical quality enabling their application in laser systems. Advantageous spectroscopic parameters of YAG:$Nd^{3+}$ crystals and characteristic for garnets high thermal and mechanical resistance results in their wide application for laser technology, as active material of diode pumped microlasers.

Table 5. Investigation results of pulses generation by side pumped „slabs".

| | SLAB TR | SL1/1 | SL1/2 | SL3/1 | SL3/2 | SL3/3 | SL3/4 |
|---|---|---|---|---|---|---|---|
| Crystal No. | TR | 1 | 1 | 3 | 3 | 3 | 3 |
| $Nd^{3+}$ (at.%) | 1.0 | 1.1 | 1.1 | 1.3 | 1.3 | 1.3 | 1.3 |
| $\eta$(%) | 36 | 32 | 30.5 | 32.5 | 30 | 29 | 29.6 |
| $E_{max}$ (mJ) | 17 | 15.5 | 14.3 | 15.6 | 14.3 | 13.6 | 14.1 |

## Acknowledgements

The discussed investigations have been made due to partial financial support of the State Committee for Scientific Research within the frame of PBZ 023–10 grant.

## References

1. D.P. Devor, L.G. DeShazer, and R.C. Pastor, "Nd:YAG quantum efficiency and related radiative properties", *IEEE J. Quantum Electronics* **25**, 1863–1873 (1989).
2. R.C. Powell, *Physics of Solid-State Laser Materials*, AIP Press, Springer-Verlag, New York (1998).
3. R. Fluck, M.R. Hermann, and L.A. Hackel, "Energetic and thermal performance of high-gain diode-side-pumped Nd:YAG rods", *Appl. Phys. B* **70**, 491–498 (2000).
4. Y. Kaneda and S. Kubota, "CW solid-state ultraviolet laser for optical disk mastering application", *IEEE J. Selected Topics in Quantum Electronics* **3**, 35–39 (1997).
5. F. Heine, H. Kretschmann, T. Kellner, and G. Huber, "Diode pumped, cw Nd-lasers with 4.9 watt uotput in the eyesafe region", OSA TOPS Vol. 10, *Advanced Solid-State Lasers*, 162–163 (1997).
6. P. Thony, P. Labeye, V. Marty, R. Templier, P. Besesty, and E. Molva, "1 mm single-frequency tunable microchip lasers for range finding", OSA TOPS Vol. 26, *Advanced Solid-State Lasers*, 203–207 (1999).

 